Using the Double Pulsar Eclipses to Probe Fundamental Physics

Cite as: AIP Conference Proceedings **983**, 469 (2008); https://doi.org/10.1063/1.2900276
Published Online: 04 March 2008

Rene P. Breton, Victoria M. Kaspi, Michael Kramer, et al.

Using the Double Pulsar Eclipses to Probe Fundamental Physics

Rene P. Breton*, Victoria M. Kaspi*, Michael Kramer†, Maura A. McLaughlin**,‡, Maxim Lyutikov§, Scott M. Ransom¶, Ingrid H. Stairs‖, Robert D. Ferdman‖ and Fernando Camilo††

*McGill University, Montreal, QC H3A 2T8, Canada
†University of Manchester, Manchester, M13 9PL, UK
**West Virginia University, Morgantown, WV 26506, USA
‡National Radio Astronomy Observatory, Green Bank, WV 24944, USA
§Purdue University, West Lafayette, IN 47907, USA
¶National Radio Astronomy Observatory, Charlottesville, VA 22903, USA
‖University of British Columbia, Vancouver, BC V6T 1Z1, Canada
††Columbia University, New York, NY 10027, USA

Abstract. The double pulsar system exhibits unique and spectacular eclipses when pulsar A passes behind pulsar B. We present 3.5 years of eclipse monitoring which provides an unprecedented way of probing pulsar magnetospheres, geometric orientation as well as testing general relativity. The eclipse light curve of pulsar A has a rich phenomenology. This includes little observed radio frequency dependence and periodic flux modulations in phase with the rotation of pulsar B, which allow the flux to reach uneclipsed levels in narrow windows. Over the monitoring period, the eclipse profile noticeably changed and we observe a modification in the modulation behavior. We quantitatively analyzed the data using the magnetospheric synchrotron absorption eclipse model proposed by Lyutikov and Thompson under the assumption of a simple dipolar magnetic field geometry. The success of the model at reproducing the eclipse profile indicates that the magnetic field configuration is mainly dipolar at a distance of about 0.1 light-cylinder radii from pulsar B. Model fitting leads to the determination of pulsar B's geometric orientation. Therefore by investigating the time evolution of the eclipse profile we can quantitatively test the effects of relativistic spin precession on pulsar B, as predicted by general relativity. Also, we note some peculiar features in the egress that are not well modelled and could potentially help to understand distortions of the magnetic field at the magnetosphere boundary.

Keywords: Double pulsar, eclipses, relativistic spin precession, pulsar magnetosphere
PACS: 97.60.Gb, 95.30.Sf, 04.80.Cc

INTRODUCTION

The double pulsar already provided numerous scientific results for testing general relativity and more general theories of gravity as well as putting better constraints on the rate of double neutron star mergers and giving new insights on binary pulsar evolution [see 1, 2, 3]. The rich phenomenology of the double pulsar also offers tools to investigate fundamental pulsar physics such as magnetospheric phenomena via the interaction of the two pulsars.

One of these tools is the eclipse of the 23-ms pulsar, dubbed A, when it passes behind its slower 2.8-s companion, B. It was soon recognized that the eclipses of pulsar A must originate somewhere in the vicinity of pulsar B and could therefore provide an excellent way of studying its magnetosphere.

In this paper, we present the latest results from our double pulsar eclipse study. In particular, eclipse modeling provides a new way of precisely determining the orientation of pulsar B in space and quantitatively measuring the rate of relativistic precession of its spin axis, as predicted by general relativity. It also yields direct evidence that its magnetic field geometry is predominantly dipolar.

OBSERVATIONS AND DATA REDUCTION

PSR J0737-3039 was observed with the Green Bank Telescope using the SPIGOT instrument. The receiver's bandwidth was 100 MHz centered at a central frequency of 820 MHz. A total of 51 eclipses were observed over a 3.5-year time span extending from December 2003 to April 2007. Most of the time, we recorded two or three consecutive eclipses during 5-7 hr long observations that were grouped over few-day observing campaigns. We also obtained complementary observations centered at 325, 427 and 1950 MHz.

CP983, *40 Years of Pulsars−Millisecond Pulsars, Magnetars, and More,*
edited by C. G. Bassa, Z. Wang, A. Cumming, and V. M. Kaspi,

We folded the raw data at the spin period of pulsar A using the Presto and Sigproc software packages so that, on average, four pulses of A were stacked per time interval. Then, for each interval, we measured the pulsed flux intensity, calculated the orbital phase and determined the spin phase of pulsar B.

ECLIPSE PHENOMENOLOGY

From the beginning, Lyne et al. [2] and Kaspi et al. [4] realized that the eclipses were only slightly radio-frequency dependent, becoming shorter at higher frequencies. This indicates that the eclipsing material must remain opaque over a wide range of radio frequencies. What makes the eclipses unique is that short time scale intensity variations are seen, as shown by McLaughlin et al. [5]. They also discovered that these modulations of pulsar A's flux are synchronized with the spin phases of pulsar B, indicating an important interaction between the two pulsars.

In this follow-up study of the eclipses, we searched for modulations at other radio frequencies and tried to quantify them using dynamic power spectra. This technique consists in taking Fourier transforms in a small window that is translated over the time series. This allows us to detect periodic variability in noisy data and determine the location of non-stationary spectral content. Because the modulation is relatively high frequency, we removed the overall eclipse trend by high-pass filtering the data before obtaining dynamic spectra.

We detected modulations at all radio frequencies at which observations were conducted and thus we concluded that they are generic to the eclipse phenomenon. Figure 1 shows a sample dynamic spectrum for the combined eight eclipses that were observed at 820 MHz near MJD 54200. Note that most of the power is harmonically related to the spin frequency of pulsar B with the main content in the fundamental and the first harmonic, as indicated by the black lines. Also, modulations are not found outside the eclipse, which spreads $\pm 1^\circ$ around conjunction. The power content switches from a mode at twice the frequency of B to one time per rotation. This mode switching is easily visible when we fold the eclipse light curve at the period of pulsar B as showed in Figure 2.

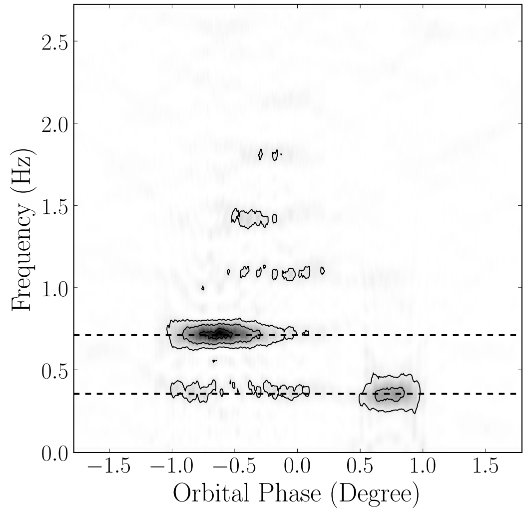

FIGURE 1. Dynamic power spectrum analysis of the combined eight eclipses observed at epoch MJD 54200. The figure shows the spectral energy density, vertically, as a function of orbital phase. Data were high-pass filtered in order to remove the low-frequency eclipse trend. The dashed lines indicate the fundamental and the first harmonic of pulsar B's spin frequency at 0.36 and 0.72 Hz, respectively. Contours identify constant power density levels.

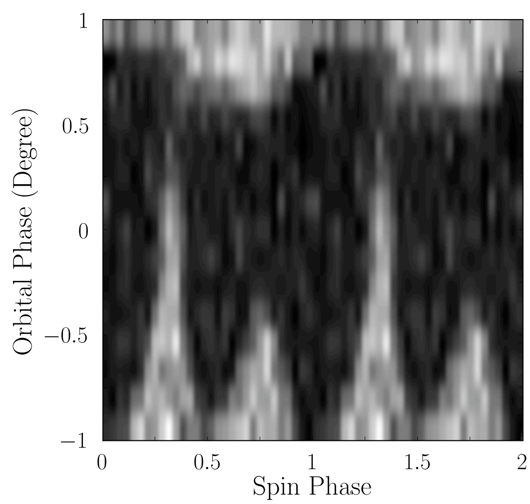

FIGURE 2. Folded eclipse profile for the eight eclipses observed at epoch MJD 54200. Eclipses were combined before being folded at the spin period of pulsar B. Lighter regions have higher flux intensity levels.

ECLIPSE MODELING

Lyutikov and Thompson [6] proposed an explanation for the flux modulation visible in the eclipses. In their model, radio emission from pulsar A is absorbed via synchrotron resonance with relativistic electrons trapped in the magnetosphere of pulsar B. This process is efficient over a wide range of radio frequency and hence explains the lack of radio frequency dependence in the eclipse profile. Since synchrotron opacity is a function of plasma density and the strength and direction of the magnetic field, it is obvious that attenuation of the radio emission from pulsar A must be related to the spin phase of pulsar B.

As described in Section 5 of Lyutikov and Thompson [6], the magnetosphere geometry is chosen to be a dipole having a misalignment χ with respect to the spin axis. This dipole magnetic field is truncated at some radius $R_{\rm mag}$, which, given the eclipse duration, is of the order of $1/10$ of the light-cylinder radius. The absorbing plasma trapped within the closed field lines of this dipole has a fixed density along constant field lines.

We define the orientation of pulsar B's spin axis using a coordinate system centered on pulsar B, as shown in Figure 1 of Lyutikov and Thompson [6], where the x-axis points toward the Earth and the y-axis is parallel to the motion of pulsar A projected onto the sky plane. Because the orbital inclination is very close to 90°, the z-axis is coincident with the orbital angular momentum and the x-y plane is parallel to the orbital plane. Therefore, the orientation of pulsar B's spin axis can be described by θ and ϕ, the colatitude of the spin axis with respect to the orbital angular momentum and the longitude of the spin axis, respectively.

Finding the best-fit model parameters requires solving a multidimensional inverse problem involving the orientation of pulsar B in space. Fitting was first performed using a Markov Chain Monte Carlo algorithm coupled to simulated annealing to boost the efficiency of the parameter space search. We mapped the likelihood over the entire parameter space and found only one set of possible geometrical configurations. The second step involves a fine grid search of the $\theta - \phi - \chi$ parameter sub-space centered on the region of maximum likelihood. This allows us to determine with high precision the most probable orientation of pulsar B for each one of the 51 eclipses in our data set.

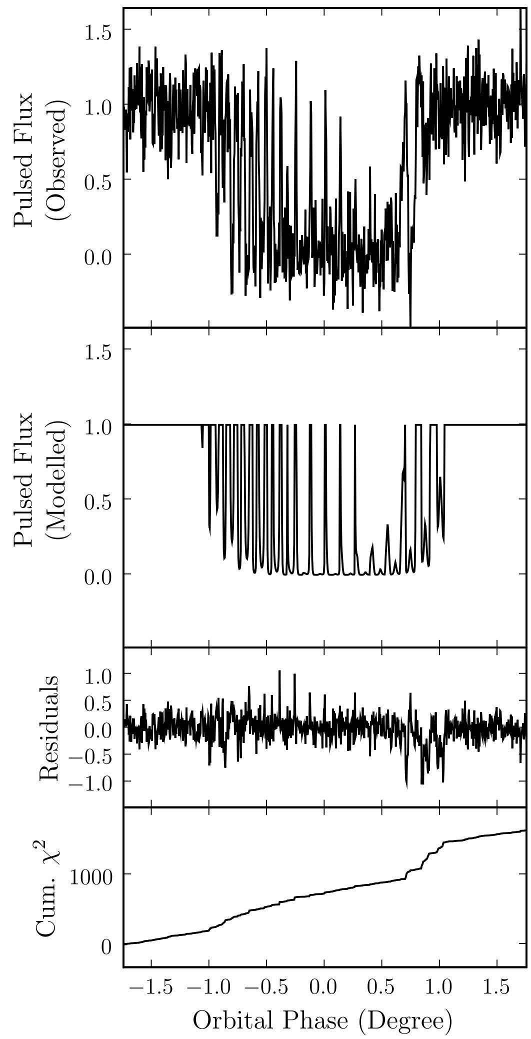

FIGURE 3. Sample fit results for the combined eight eclipses at epoch MJD 54200 showing the observed pulsed flux intensity, the modeled pulsed flux intensity, the weighted fit residuals and the cummulative χ^2 from top to bottom, respectively.

FITTING RESULTS

Figure 3 shows the fit results for the combined eight eclipses that were observed at epoch MJD 54200. The model light curve is able to reproduce extremely well most of the features that are seen in the combined eclipse profile, and especially the transition from the double to single modulation feature per rotation of pulsar B. The post-fit residuals are relatively featureless although we observe that the eclipse egress is not fitted perfectly. This is easily visible as a jump in the cumulative χ^2. Possible reasons are a more complicated plasma density distribution near the magnetosphere boundary where the opacity rises rapidly, or a slight distortion of the magnetosphere itself. Because the center of the eclipse and, in particular, the location of the transition from double to single modulation are the most important elements determining the orientation, we discarded from the fit the egress section where the cumulative χ^2 shows a clear break.

The key ingredients to successful modeling are a sharp opacity transition at the magnetosphere boundary and the condition that the absorbing plasma is trapped within the closed field lines of a truncated dipole. That is, the equation for last closed field line is $R_{\rm mag} = r/\sin^2\theta_\mu$, where

θ_μ is the magnetic colatitude. We find that these two conditions drive the position and the width of the features seen in the profile. Details of the exact magnetic field orientation within the closed field lines as well as the exact plasma density distribution are second order effects. This is because probing the inner magnetosphere is difficult as the opacity rises very quickly. Discrepancies are larger on the edge of the magnetosphere, where the plasma column density is smaller, but given the limited instrument sensitivity, these subtle effects are difficult to disentangle from simple noise fluctuations. Finally, as pointed out by Lyutikov and Thompson [6], the success of the model at reproducing the eclipses is very strong empirical evidence that the pulsar magnetic field structure is dipolar, at least on the considered spatial scale.

ECLIPSE EVOLUTION

The double pulsar eclipses offer a wonderful new tool to investigate changes in the system geometry. General relativity predicts that spin-orbit coupling causes the spin angular momentum vector of pulsar B to precess around the system's total angular momentum vector with a period of 71 years. This relativistic spin precession of pulsar B should be the dominant effect leading to an evolution of the eclipse profile. We can therefore use the results from eclipse the fitting to quantitatively measure changes in the geometry. In our model framework this means that $\phi \to \phi(t) = \Omega_B t + \phi_0$, with the expected rate of change $|\Omega_B| = 5.07^\circ\,\mathrm{yr}^{-1}$ as predicted by general relativity.

Qualitatively, there are visible signs that the eclipse profile has evolved over the last 3.5 years. Figure 4 shows the average profile at different epochs. We clearly see that some prominent features appeared in the eclipse egress. We also observe that the transition from double to single modulation and the orbital phase at which these features disappear is slowly drifting with time from the egress toward the ingress.

Measurement of the best-fit geometry at different epochs allows us to quantitatively assess that the magnetic inclination angle, χ, and the colatitude of the spin axis, θ, do not significantly vary as a function of time. On the other hand, the longitude of the spin axis, ϕ, appears to be time-dependent. We draw these conclusions from linear fits of θ, χ and ϕ after marginalizing the three-dimensional $\theta - \chi - \phi$ likelihood space down to the dimension of interest.

The best way of investigating the time evolution of the longitude of spin axis is to embed the individual eclipse modeling in a "super eclipse model" in which we simultaneously fit constant θ and χ values while searching for the best linear change in ϕ. Performing a joint fit is more reliable since it preserves information about correlation between parameters.

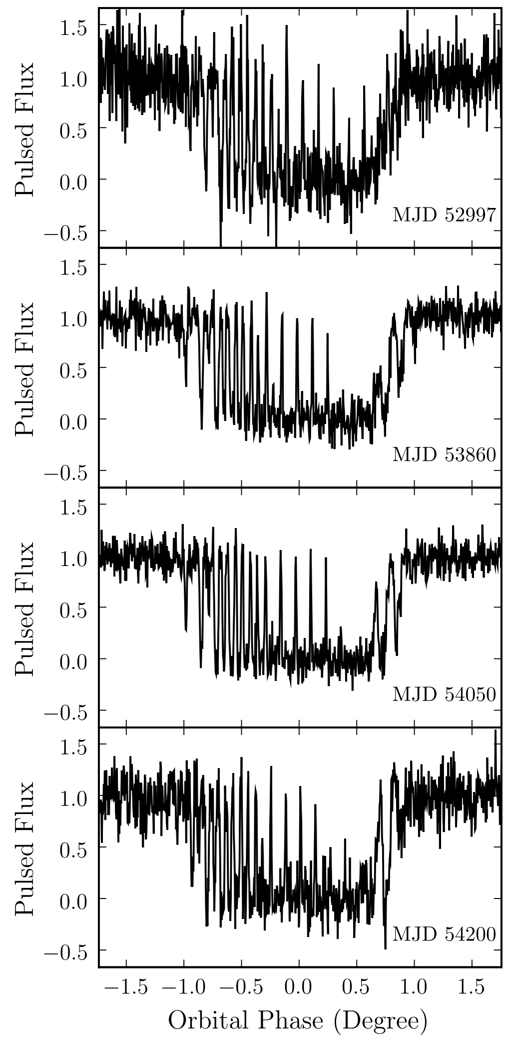

FIGURE 4. Evolution of the average eclipse profile at different epochs. A total of 3, 8, 13 and 8 individual eclipses were combined to make the profiles at MJD 52997, 53860, 54050 and 54200, respectively.

Results from the joint fit are illustrated in Figure 5. We find that $\theta_0 \sim 130^\circ$, $\chi_0 \sim 70^\circ$ and $\phi_0 \sim 55^\circ$[1]. General relativity predicts that the longitude of spin axis should change at a rate $|\Omega_B| = 5.07^\circ\,\mathrm{yr}^{-1}$. From the posterior density probability of this parameter, we derive a relativistic spin precession rate that is in agreement with general relativity.

[1] These are preliminary results. The final analysis will be presented in a forthcoming paper

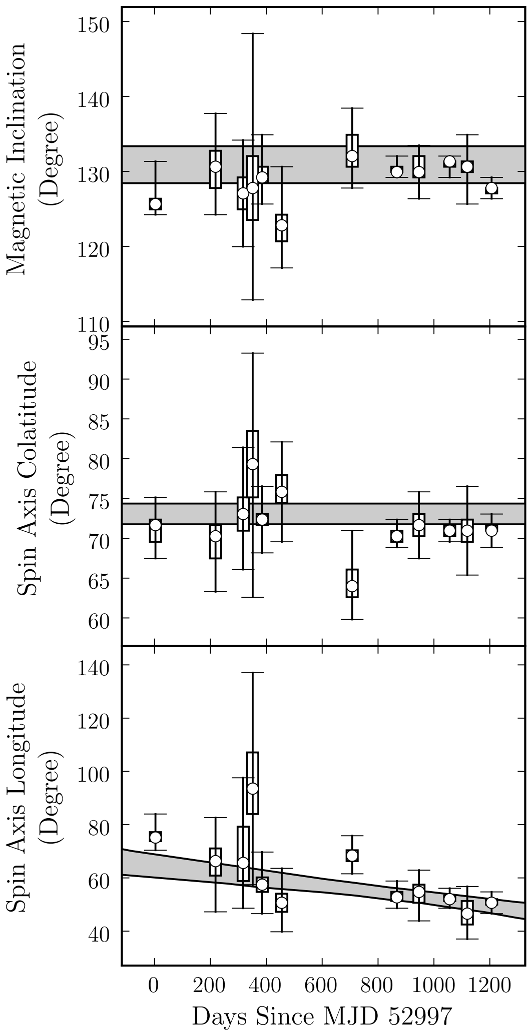

FIGURE 5. Evolution of pulsar B's geometry as a function of time. The marginalized posterior probability distribution of the magnetic inclination (χ), the colatitude of the spin axis (θ) and the longitude of the spin axis (ϕ) of pulsar B are shown from top to bottom, respectively. For each data point, the circle represents the median value of the posterior probability density while the box and the bar indicate the 1 and 3σ confidence intervals, respectively. The gray regions are the 3σ confidence regions determined from the joint-fit model $\mathscr{L}(\theta : \theta_0, \chi : \chi_0, \phi : \Omega_B t + \phi_0)$.

CONCLUSIONS

The eclipses of pulsar A in the double pulsar system are unique in that the observed flux is modulated by the rotation of the other pulsar. Although the eclipse light curves show a complex phenomenology, they are successfully explained by a relatively simple interaction with relativistic plasma trapped in the closed field lines of a truncated dipole. The remarkable match of this model with the observations suggests strong empirical evidence that pulsars predominantly have dipolar magnetic fields, at least on a scale $\sim 10\%$ the nominal light-cylinder radius, as pointed by Lyutikov and Thompson [6].

Moreover, our model fitting is accurate enough to constrain the orientation of pulsar B in space and detect the secular change of its spin axis longitude on a 3.5-yr time scale. This effect is associated with relativistic spin precession, as predicted by general relativity. We measure the magnitude of the rate of change to be in excellent agreement with the value $5.07^\circ\,\mathrm{yr}^{-1}$ expected if general relativity is correct. In the future, a longer time baseline may keep improving these results and provide valuable new way of testing theories of gravity in the strong field regime.

ACKNOWLEDGMENTS

Funding for this work was provided by NSERC Discovery Grant Rgpin 228738-03, Fonds de Recherche de la Nature et des Technologies du Québec, the Canadian Institute for Advanced Research and the Canada Foundation for Innovation. V.M.K. holds a Canada Research Chair and the Lorne Trottier Chair in Astrophysics and Cosmology. The Green Bank Telescope is part of the National Radio Astronomy Observatory, a facility of the National Science Foundation operated under cooperative agreement by Associated Universities, Inc.

REFERENCES

1. M. Burgay, N. D'Amico, A. Possenti, R. N. Manchester, A. G. Lyne, B. C. Joshi, M. A. McLaughlin, M. Kramer, J. M. Sarkissian, F. Camilo, V. Kalogera, C. Kim, and D. R. Lorimer, *Nature* **426**, 531–533 (2003).
2. A. G. Lyne, M. Burgay, M. Kramer, A. Possenti, R. N. Manchester, F. Camilo, M. A. McLaughlin, D. R. Lorimer, N. D'Amico, B. C. Joshi, J. Reynolds, and P. C. C. Freire, *Science* **303**, 1153–1157 (2004).
3. M. Kramer, I. H. Stairs, R. N. Manchester, M. A. McLaughlin, A. G. Lyne, R. D. Ferdman, M. Burgay, D. R. Lorimer, A. Possenti, N. D'Amico, J. M. Sarkissian, G. B. Hobbs, J. E. Reynolds, P. C. C. Freire, and F. Camilo, *Science* **314**, 97–102 (2006).
4. V. M. Kaspi, S. M. Ransom, D. C. Backer, R. Ramachandran, P. Demorest, J. Arons, and A. Spitkovsky, *ApJ* **613**, L137–L140 (2004).
5. M. A. McLaughlin, A. G. Lyne, D. R. Lorimer, A. Possenti, R. N. Manchester, F. Camilo, I. H. Stairs, M. Kramer, M. Burgay, N. D'Amico, P. C. C. Freire, B. C. Joshi, and N. D. R. Bhat, *ApJ* **616**, L131–L134 (2004).
6. M. Lyutikov, and C. Thompson, *ApJ* **634**, 1223–1241 (2005).